

Extensibility and Recovery in a Crystalline–Rubbery–Crystalline Triblock Copolymer

Sasha B. Myers[†] and Richard A. Register*

Department of Chemical Engineering, Princeton University, Princeton, New Jersey 08544-5263.

[†] Current address: 3M Corporate Research Process Laboratory, St. Paul, MN 55144.

Received May 17, 2009; Revised Manuscript Received June 17, 2009

ABSTRACT: The synthesis, morphological characterization, and deformation behavior of a triblock copolymer containing linear polyethylene (LPE) end blocks and a hydrogenated polyhexylnorbornene (hPHN) midblock are presented. The block copolymer forms a homogeneous melt; upon cooling, LPE crystallization creates a lamellar structure consisting of alternating “hard” semicrystalline LPE domains and “soft” rubbery hPHN domains, imparting thermoplastic elastomer (TPE) behavior to the material. At 20 wt % LPE, the triblock shows a low modulus, high ultimate strain, and excellent strain recovery compared with other crystalline-block TPEs. Though the LPE crystals fragment upon deformation, the interposing hPHN layers hinder LPE fragments originating in different layers from fusing together, preserving the memory of the original domain morphology to high strains.

Introduction

While thermoplastic elastomers (TPEs) are much more easily processed (and reprocessed) than covalently cross-linked elastomers, their use is frequently limited by incomplete recovery from large deformations, commonly referred to as “permanent set”. This irrecoverable deformation implies a substantial rearrangement of the material’s microscopic morphology under load—a structural impermanence of the physical cross-links which anchor the elastomeric chains at room temperature. Perhaps the best-known TPEs are ABA triblock copolymers with glassy end blocks (A) and a rubbery midblock (B); typically, A is polystyrene and B is a polydiene or amorphous hydrogenated polydiene.¹ To achieve elastomeric behavior, the A block is the minority component, so microphase separation forms glassy A spheres or cylinders which act as the physical cross-links for the rubbery B midblock chains. Such polymers will often recover nearly completely from modest strains (<50%), and while some permanent set is observed following larger strains, their primary limitations are their poor solvent resistance and the relatively high viscosities and elasticities of their microphase-separated melts.

Alternatively, crystalline polymers can be used as the “hard” blocks. Well-known examples are segmented poly(ether–ester) multiblock copolymers,² where the “hard” blocks are typically semicrystalline poly(tetramethylene terephthalate) and the “soft” blocks are typically rubbery poly(tetramethylene oxide). Compared with polystyrene-based TPEs, these PTMT–PTMO multiblock copolymers show excellent solvent resistance; moreover, at the short segment lengths used, these polymers form homogeneous (disordered) melts which are easily processed.³ The microphase-separated structure present at room temperature is thus driven entirely by hard-block crystallization.³ A drawback of such materials is that the soft segment molecular weight is limited, so relatively high hard segment contents are required to maintain sufficiently high melting and freezing points; the resulting TPEs have relatively high moduli and exhibit considerable permanent

set when strained outside the initial elastic region (above ≈10% strain).²

An attractive option would be to combine the best features of both classes of materials, by synthesizing block copolymers having a relatively small number of long blocks (as in the styrene–diene materials), but where the “hard” blocks are semicrystalline (as in the PTMT–PTMO multiblocks), conferring solvent resistance and small block incompatibility in the melt. Koo et al. have evaluated semicrystalline block copolymers with hydrogenated polybutadiene (hPBd) as the crystalline end block and hydrogenated polyisoprene (or poly(ethylene-*alt*-propylene), PEP) as the rubbery midblock.^{4,5} At sufficiently high molecular weights, ultimate strains as high as 900% were achieved, along with substantial strain hardening.⁵ Similar results were achieved by Hotta et al.⁶ using isotactic or syndiotactic polypropylene hard blocks and poly(ethylene-*stat*-propylene) or regio-irregular polypropylene soft blocks; the best of these materials further exhibited excellent recovery even from large deformations, up to 1000% uniaxial strain. Closer to the multiblock end of the spectrum, researchers at Dow Chemical have recently developed a “chain-shuttling” polymerization chemistry⁷ which can produce blocky copolymers of polyethylene and poly(ethylene-*stat*-octene). When the bulk of the chains contain 2–10 blocks, and the polyethylene hard segments are the minority component, these materials make effective TPEs, with good recovery from strains up to 300%.⁸

These examples illustrate the benefits to be captured in TPEs based on semicrystalline hard blocks: namely, the room-temperature insolubility of many crystalline polymers (including polyethylene) and the possibility to drive microphase separation purely by crystallization from an easily processed single-phase melt. The principal drawbacks to such materials result from the formation of extended or interconnected hard domains: a large small-strain modulus and poor recovery from deformation. Here, we present the synthesis and characterization of a new triblock copolymer TPE having semicrystalline linear polyethylene end blocks (LPE) and a rubbery hydrogenated poly(5-*n*-hexylnorbornene) midblock (hPHN), which shows the low initial modulus and high recovery desired in elastomers.

*Corresponding author. E-mail: register@princeton.edu.

Experimental Section

Synthesis. The LPE/hPHN/LPE triblock copolymer was synthesized by ring-opening metathesis polymerization (ROMP) of a PCP/PHN diblock (where PCP is polycyclopentene), followed by coupling to form the PCP/PHN/PCP triblock, and subsequent hydrogenation. All ROMP reactions were run under a nitrogen atmosphere in an Innovative Technologies glovebox (~ 0.7 ppm of O_2 , ~ 0.5 ppm of H_2O), with the Schrock-type initiator 2,6-diisopropylphenylimidoneophylidenemolybdenum(VI) bis(*tert*-butoxide) (Strem Chemicals, used as received). 5-*n*-Hexylnorbornene (Promerus, 77/23 mixture of endo/exo) and polymerization regulator trimethylphosphine (PMe_3) were each dried over freshly cut sodium, degassed by freeze–pump–thaw cycles, and vacuum-transferred prior to use. Cyclopentene monomer (96%, Aldrich) and toluene were each dried over diphenylhexyllithium (adduct of butyllithium and diphenylethylene), degassed by freeze–pump–thaw cycles, and vacuum-transferred. Isophthalaldehyde was degassed prior to use. The PCP block was synthesized using the method and kinetic parameters developed by Trzaska et al.⁹ The Mo initiator was added to toluene, followed by the addition of PMe_3 (5 equiv vs Mo) and cyclopentene to a concentration of 3 M. The reaction mixture was stirred for 60 min, and 5 equiv of hexylnorbornene was added. The solvent and excess monomer were then removed from the flask by vacuum transfer. The polymer chains were redissolved in toluene, followed by the addition of the remaining hexylnorbornene monomer. The reaction mixture was stirred for an additional 60 min, and 0.5 equiv of isophthalaldehyde was added.¹⁰ The mixture was stirred for an additional 30 min; the polymer was recovered, purified by repeated precipitation into methanol, and dried under vacuum at room temperature.

Hydrogenation of the PCP/PHN/PCP triblock to LPE/hPHN/LPE was carried out in a stirred Parr reactor, in cyclohexane at 0.5 wt % polymer, using a $Pd^0/CaCO_3$ catalyst (5 wt % Pd^0 , Alfa Aesar) in a 1:20 weight ratio of Pd^0 to polymer.⁹ The reaction was run at 100 °C and a minimum of 400 psig. Hydrogenation was continued for 1–3 days until the *trans* C=C double bond stretch at 966 cm^{-1} in the infrared spectrum was reduced to baseline, which corresponds to >99.95% saturation.

Molecular Characterization. Characterization was conducted on the soluble, unsaturated PCP/PHN/PCP triblock, the aliquot of the PCP/PHN precursor diblock, and the aliquot of the PCP first block. Gel permeation chromatography (GPC) in tetrahydrofuran (THF) was used to determine polymer molecular weight, using a Waters 515 HPLC pump, two 30 cm Polymer Laboratories PLgel Mixed-C columns, and a Waters 410 differential refractometer detector. The GPC columns were calibrated with narrow-distribution polystyrene standards, and the results converted to true molecular weights via division by the hydrodynamic correction factors¹¹ $R = 1.32$ for PHN¹² and $R = 1.98$ for PCP¹³ in THF. Block copolymer compositions were determined by 1H NMR, using the olefinic protons from both repeat units and the methine protons from the PHN block.

Thermal, Mechanical, and Morphological Characterization. Differential scanning calorimetry (DSC) employed a Perkin-Elmer DSC 7 equipped with an intracooler and calibrated with indium and mercury. ~ 10 mg samples were examined on heating at 10 °C/min heating after cooling from the melt at 10 °C/min. The room-temperature mechanical properties of the triblocks were measured by uniaxial tensile testing. Samples were prepared by melt-pressing into sheets (~ 0.7 mm in thickness) from which ASTM D1708 dogbones were stamped; tests were run on an Instron 5865, at 2 in./min (initial strain rate = 0.038 s^{-1}). Strains are calculated based on crosshead displacement and are presented relative to the initial specimen length; except where noted, stress values quoted are engineering stresses (i.e., relative to the initial specimen cross section). Transmission wide- and small-angle X-ray scattering (WAXS and SAXS) employed two

systems run from a common PANalytical PW3830 generator with long fine focus Cu X-ray tube to yield Cu K α radiation. WAXS measurements employed a Statton pinhole camera system previously described,¹⁴ using Kodak image plates read by a GE Biosciences Storm 820 scanner. SAXS measurements employed an Anton-Paar compact Kratky camera with hot stage and an MBraun OED-50 M position-sensitive detector. Data were corrected for detector sensitivity and positional linearity, empty beam scattering, and sample thickness and transmittance, placed on an absolute intensity scale via a polyethylene standard, and desmeared for slit length.¹⁵ Intensities are presented against the magnitude of the momentum transfer vector $q = (4\pi/\lambda) \sin \theta$, where θ is half the scattering angle; calibration was via silver behenate¹⁶ ($d = 5.838\text{ nm}$).

Results and Discussion

Synthesis of the LPE/hPHN/LPE triblocks required a multi-step procedure: synthesis of a PCP/PHN diblock, coupling of the diblock to form the PCP/PHN/PCP triblock, and hydrogenation to LPE/hPHN/LPE, as shown in Figure 1. Once the living PCP block had grown to the target length, it was “capped” by adding 5 equiv (vs Mo initiator) of hexylnorbornene monomer to convert essentially all chain ends from PCP to PHN. The higher ring strain of the bicyclic hexylnorbornene monomer ensures a negligible depropagation rate during the subsequent steps, unlike living PCP, which can be completely depolymerized under vacuum.¹⁷ The solvent (toluene) and excess cyclopentene monomer were then removed by vacuum, leaving the living PHN-capped chains, to which new solvent (toluene) and the remaining hexylnorbornene monomer charge were added. Finally, isophthalaldehyde was added to couple the chains.¹⁰ Coupling ensures that the two PCP end blocks are statistically identical; though the coupling step could be replaced with the addition of a second charge of cyclopentene to generate a PCP/PHN/PCP triblock, the limited conversion of cyclopentene to polymer would make it difficult to precisely match the two end block lengths.⁹

A PCP/PHN/PCP triblock was synthesized with target block molecular weights of 10/80/10 kg/mol (20 wt % end block). GPC traces of aliquots taken at intermediate steps are shown in Figure 2. The PCP first block (green curve) is narrowly distributed, with a high molecular weight shoulder resulting from acyclic metathesis events which generate “telechelic” chains bearing a catalyst site at each end.¹⁸ The absolute number-average molecular weight of the PCP first block is 11.5 kg/mol. After growth of the hexylnorbornene block (orange curve), the distribution remains narrow. The triblock product (black curve) contains primarily the triblock of interest (PCP/PHN/PCP), at precisely double the molecular weight of the PCP–PHN diblock. The small high-molecular-weight peak again results from the difunctional propagating chains (coupling, statistically, with two monofunctional chains), while the small low-molecular-weight peak reflects PCP/PHN diblocks which failed to couple. Since these minor components have very similar PCP:PHN ratios as the principal triblock product, they were not removed. 1H NMR indicated a PCP weight fraction of 0.197, yielding an LPE weight fraction of 0.203 upon complete hydrogenation; the number-average molecular weight of the fully saturated triblock is thus 12/93/12 kg/mol. Alternatively, the block molecular weights may be determined from GPC alone, since the hydrodynamic correction factors R are known for both PCP and PHN; this method yields a triblock molecular weight of 12/87/12 kg/mol (21 wt % LPE), in good agreement with the direct 1H NMR measurement.

DSC revealed a glass transition at $T_g = -17\text{ °C}$, near that of hPHN homopolymer¹² (-22 °C), and a unimodal LPE melting endotherm with a peak temperature of 121.6 °C and an enthalpy of 36 J/g triblock, which equates to an LPE weight fraction

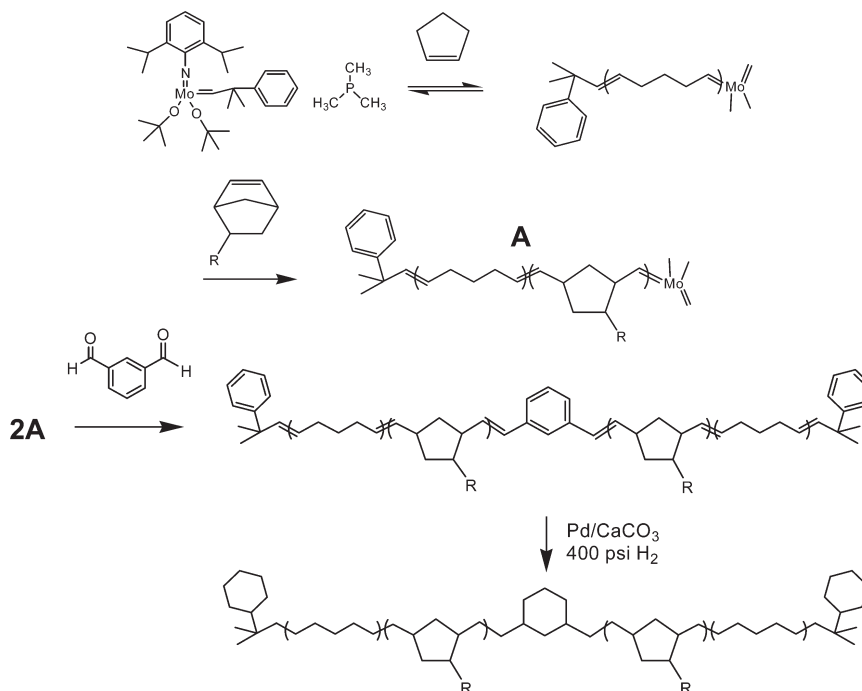


Figure 1. Schematic for the triblock synthesis. Mo-initiated sequential ROMP of cyclopentene and hexylnorbornene yields a PCP/PHN diblock, which is then coupled to yield a PCP/PHN/PCP triblock that is subsequently hydrogenated to LPE/hPHN/LPE. Here, the side chain R is *n*-hexyl.

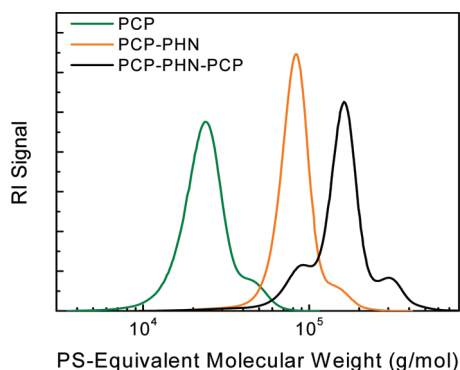


Figure 2. GPC chromatograms for PCP/PHN/PCP after each major reaction step. The final reaction product (black curve) contains primarily the triblock, with some acyclic metathesis products at high molecular weight and some uncoupled diblock at low molecular weights. Molecular weights are expressed relative to the molecular weight of a linear polystyrene calibrant with the same elution time; absolute molecular weights may be obtained through the appropriate hydrodynamic correction factor, as discussed in the text.

crystallinity $w_c = 0.64$. In LPE homopolymer, a melting point of 121.6°C translates to¹⁹ a crystal thickness $t_c = 10.9$ nm. Note that these values of crystallinity, melting point, and crystal thickness are all significantly greater than those achievable when hydrogenated low-vinyl polybutadiene (hPBd) is employed as the “polyethylene” block, since the ethyl branches severely limit these quantities (to $w_c \approx 0.35$, $T_m \approx 100^\circ\text{C}$, $t_c \approx 6$ nm).^{4,5,20–22}

SAXS patterns for the triblock are shown in Figure 3. The melt-phase pattern (140°C) shows no peaks, consistent with a homogeneous melt; we calculate¹³ an electron density difference $\Delta\rho_e > 12\text{ e}/\text{nm}^3$ between molten LPE and hPHN at 140°C , which would yield more than adequate contrast to reveal any microphase separation in the melt. Upon slow cooling to room temperature, the SAXS pattern develops a principal reflection at $q^* = 0.148\text{ nm}^{-1}$ (Bragg spacing $d = 2\pi/q^* = 42.5$ nm). The broad shoulder at $q > q^*$, followed by the minimum at $q_{\min} = 0.68\text{ nm}^{-1}$, is consistent with the form-factor scattering from

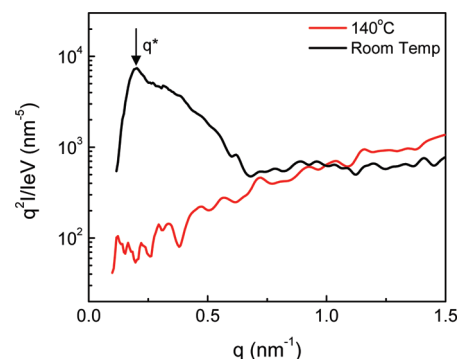


Figure 3. SAXS patterns in the melt (red) and at room temperature (black) for the LPE/hPHN/LPE triblock.

lamellae²³ of uniform thickness $t = 9.2$ nm, in reasonable agreement with the value of the LPE layer thickness calculated assuming complete phase separation (8.4 nm), and the value of t_c estimated above from the melting point by comparison with LPE homopolymers (10.9 nm). The fact that the triblock's T_g is close to that of hPHN homopolymer implies that the uncrystallized LPE fraction remains closely associated with the LPE crystals, rather than mixing homogeneously with the hPHN. Taken together, these results indicate that crystallization of this LPE/hPHN/LPE triblock from a homogeneous melt yields a cleanly microphase-separated lamellar structure consisting of semicrystalline LPE layers and amorphous hPHN layers in a thickness ratio of 1:4.

The mechanical properties of the triblock were evaluated by uniaxial tensile testing. The stress–strain response for the triblock is shown in Figure 4, in terms of both engineering stress σ_{engr} and true stress σ_{true} ; since the deformation was observed to be homogeneous throughout the gauge length, the measured engineering stress can be converted to true stress simply as $\sigma_{\text{true}} = \sigma_{\text{engr}}(1 + \epsilon/100)$, where ϵ is the percent strain, assuming that Poisson's ratio is 1/2. The small-strain tensile modulus of the LPE/hPHN/LPE triblock is measured as 10 MPa, well below the

range of typical poly(ether-ester) semicrystalline multiblock copolymers² and comparable to that of styrenic triblock copolymers possessing a cylindrical hard domain morphology.²⁴ The plot of σ_{engr} shows a distinct broad maximum near $\varepsilon = 370\%$; at this same value of ε , the plot of σ_{true} begins to plateau, indicating yielding of the hard domains. By the Considère construction,²⁵ necking occurs when σ_{true} (not σ_{engr}) exhibits a maximum, consistent with the fact that no neck was observed near 400% strain. The plot of σ_{true} does show a weak maximum near $\varepsilon = 750\%$; while the formation of a shallow neck at these high strains is possible, it is more likely that this feature is simply a consequence of the fact that the test is conducted at a constant crosshead displacement rate, which translates to a progressively decreasing strain rate. The plateau value in σ_{true} is set by the yield

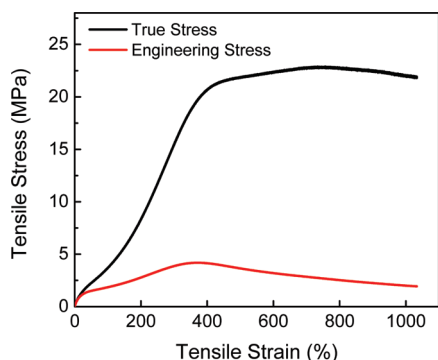


Figure 4. Room-temperature tensile stress-strain curves for the LPE/hPHN/LPE triblock, presented as both engineering stress (red) and true stress (black). Test was conducted at a constant crosshead displacement, corresponding to an initial strain rate of 0.038 s^{-1} .

strength of the LPE crystals, which at room temperature is $\sim 25 \text{ MPa}$ for PE crystals 10 nm thick.²⁶

The triblock's strain recovery behavior was examined next. Upon stretching the polymer to 200% strain and unloading, we observed nearly complete recovery, as shown in Figure 5a. This procedure was repeated with a 5 min recovery time between runs. The first run showed a small amount of irrecoverable plastic deformation, but in the second and third cycles, very little permanent change in sample length was observed. Moreover, there is little change in the shape of the stress-strain curve even between the first and second cycles, implying little change in the hard domain continuity. This is remarkable, considering that the physical cross-links in our polymers are PE crystals; for PE homopolymers and statistical copolymers, cyclic tests such as those in Figure 5a invariably lead to high degrees of permanent set, except at very small strains ($<10\%$).²⁷ Upon repeated stretching to higher strain (400% elongation, just past the maximum in σ_{engr}), we observe noticeably more plastic deformation (Figure 5b), but the fractional recovery is still quite high. As in the 200% strain cycle experiment, most permanent deformation happens on the first run; subsequent runs show much smaller incremental decreases in recovery. However, at such large deformations, there is a substantial change in the shape of the curve between the first and second cycles, leading to a substantially lower stress at all strains; even in subsequent cycles, the maximum stress progressively drops. These changes indicate a progressive fragmentation of the hard domains (LPE crystals) at 400% applied strain, though at 200% applied strain, the hard domains are quite stable.

For ease of comparison, the data are presented as fractional recovery in Figure 5c. Note that 200% strain leads to only 1% of applied strain unrecovered (2% permanent set based on initial specimen length), with this value increasing to only 5.5%

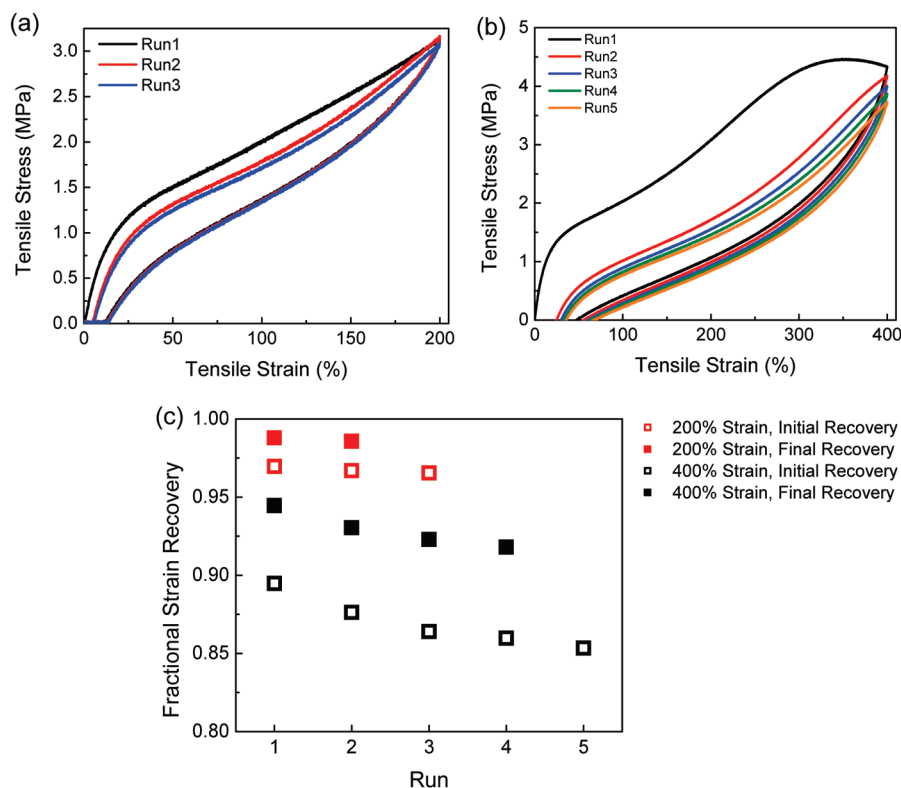


Figure 5. Tensile curves after straining LPE/hPHN/LPE to (a) 200% and (b) 400% in cycles with a 5 min hold time between runs. (c) Summary of fractional strain recovery for both data sets; “initial recovery” values are derived from the strain value where the stress returns to zero during the cyclic test, while “final recovery” values are derived from the strain value 5 min later.

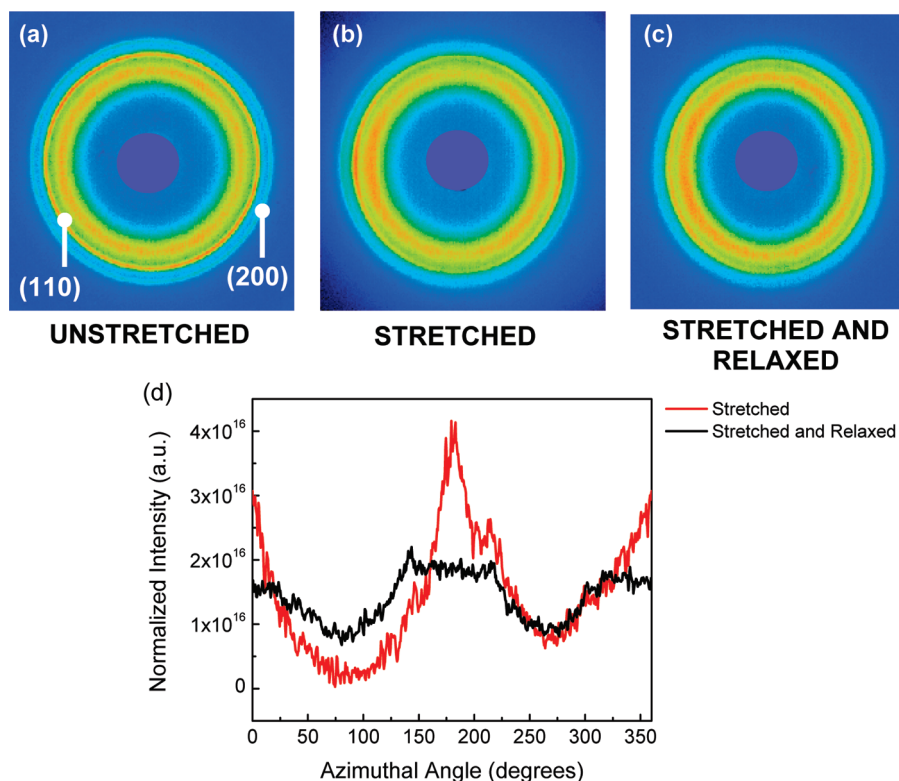


Figure 6. 2D WAXS patterns of LPE/hPHN/LPE triblock (a) before tensile testing, (b) while stretched to 600%, and (c) relaxed after stretching to 1030%. (d) Azimuthal intensity profiles for the (110) peak for the two deformed specimens, showing strong orientation at 600% strain (red) and substantial recovery upon unloading even from 1030% strain (black). Stretch direction is vertical in all images; in (d), equator corresponds to 0°.

unrecovered at 400% strain (22% permanent set). These values are comparable to those for commercial styrenic TPEs; for example, a polystyrene–poly(ethylene-*stat*-butylene)–polystyrene triblock copolymer with 29 wt % styrene and a total molecular weight of 50 kg/mol (Kraton G1652) shows a fractional strain recovery of 98% following a 300% strain (2% of applied strain unrecovered). For our LPE/hPHN/LPE triblock, even after four cycles to 400% strain, only 8% of the applied strain amplitude is unrecovered. All these recoveries far exceed those observed with typical segmented poly(ether-ester)s, which have a higher degree of hard domain connectivity.² A more direct comparison can be made with the polyolefin starblock copolymers of Ver Strate et al.,²⁸ which have LPE outer blocks and poly(ethylene-*stat*-propylene) inner blocks; with an LPE content of 44 wt %, they obtained thermoplastic elastomer behavior, but with a 9% permanent set following only 100% deformation. Wang et al.⁸ have clearly shown how permanent set increases with hard block content in multiblock copolymers of polyethylene and poly(ethylene-*stat*-octene); at hard block contents of 20 wt %, comparable but slightly poorer recoveries are observed as for our LPE/hPHN/LPE triblock (20 wt % hard block). The recovery behavior of this LPE/hPHN/LPE triblock following 200% and 400% strain exceeds even that of the triblock and pentablock copolymers of isotactic polypropylene and regioirregular polypropylene examined by Hotta et al.⁶

The high degree of macroscopic recovery implies a similar recovery of the microscopic structure, which we examined more directly by two-dimensional wide-angle X-ray scattering. 2D WAXS patterns for the triblock are shown in Figure 6, captured with the beam perpendicular to the stretching direction, which is vertical in all images. The first image shows the pattern taken prior to deformation. Starting from the center, the rings correspond to the amorphous chains, the (110) reflection of orthorhombic PE, and the corresponding (200) PE reflection; the uniform intensity distribution around each ring indicates

complete isotropy of both the amorphous phase and the crystals. The second pattern was captured while the sample was stretched and held at ~600% strain and shows the intensity for all rings concentrated on the equator. This indicates preferred orientation of both the amorphous segments and crystals, with the chain axes aligned in the stretching direction. Upon further stretching to 1030% strain—just short of the breaking point—then unloading the specimen and allowing it to relax, the third pattern was captured; it shows only partial recovery, consistent with the substantial permanent set (280%, or 27% of applied strain) measured on the same specimen. Though this represents much poorer recovery than from 200 or 400% applied strain, it is still substantial; since the yield point of the LPE crystals occurs near 370% strain, the subsequent strain beyond this point is 660%, more than half of which is recovered upon unloading. This contrasts with the behavior of PE homopolymers and copolymers, where essentially all applied strain beyond 80% is unrecovered upon unloading.²⁷

Panel d of Figure 6 shows the azimuthal intensity profiles for the (110) reflection for the two deformed specimens. This illustrates more clearly that most of the orientation imparted by elongation, even up to the breaking point, is largely recovered upon unloading. The high degree of orientation of the (110) and (200) reflections at 600% strain reflects the fragmentation of the LPE lamellae (“coarse slip”), as is found in PE homopolymers and statistical copolymers, where a “fibrillar” texture starts to develop around 80% strain.²⁷ But in such materials, relative motion of adjacent fibrils allows fragments derived from different crystallites to fuse together, generating a new crystalline superstructure which does not spontaneously break apart when the stress is removed, leading to the substantial permanent set which accompanies large deformations in PE homopolymers and statistical copolymers. In our triblocks, this “fusion” of fragments is hindered by the fact that the LPE crystals are separated by the relatively thick hPHN layers, so compared with

PE homopolymers or statistical copolymers, fragments would need to be translated much greater distances to “find” a fragment originating from a different lamella. Consequently, much greater strains are required for such “fusion” events to be substantially frequent, or stated alternatively, the permanent set at a given strain will be much smaller.

Conclusions

A crystalline–rubbery–crystalline block copolymer comprised of LPE end blocks and an hPHN midblock was synthesized via living ROMP and subsequent catalytic hydrogenation. At ~20 wt % LPE and a total molecular weight of 117 kg/mol, the triblock formed a homogeneous melt and crystallized to form an alternating LPE-hPHN lamellar morphology. The triblock showed excellent recovery from 200% strain, even after multiple cycles. At higher strains, where the true stress exceeds the yield stress of the anchoring LPE crystals, the recovery is poorer but still substantial due to separation of the LPE crystal fragments by the thicker hPHN layers.

Acknowledgment. This work was supported by the National Science Foundation, through the Polymers Program (DMR-0505940) and through a Graduate Research Fellowship to S.B. M. The authors gratefully acknowledge Drs. Andrew Bell and Dino Amoroso (Promerus LLC) for the supply of hexylnorbornene monomer.

References and Notes

- (1) Holden, G.; Legge, N. R. In *Thermoplastic Elastomers*, 2nd ed.; Holden, G., Legge, N. R., Quirk, R., Schroeder, H. E., Eds.; Hanser/Gardner Publications: Cincinnati, 1996; pp 47–70.
- (2) Adams, R. K.; Hoeschele, G. K.; Witsiepe, W. K. In *Thermoplastic Elastomers*, 2nd ed.; Holden, G., Legge, N. R., Quirk, R., Schroeder, H. E., Eds.; Hanser/Gardner Publications: Cincinnati, 1996; pp 192–225.
- (3) Veenstra, H.; Hoogvliet, R. M.; Norder, B.; Posthuma de Boer, A. *J. Polym. Sci., Part B: Polym. Phys.* **1998**, *36*, 1795–1804.
- (4) Koo, C. M.; Wu, L. F.; Lim, L. S.; Mahanthappa, M. K.; Hillmyer, M. A.; Bates, F. S. *Macromolecules* **2005**, *38*, 6090–6098.
- (5) Koo, C. M.; Hillmyer, M. A.; Bates, F. S. *Macromolecules* **2006**, *39*, 667–677.
- (6) Hotta, A.; Cochran, E.; Ruokolainen, J.; Khanna, V.; Fredrickson, G. H.; Kramer, E. J.; Shin, Y. W.; Shimizu, F.; Cherian, A. E.; Hustad, P. D.; Rose, J. M.; Coates, G. W. *Proc. Natl. Acad. Sci. U. S. A.* **2006**, *103*, 15327–15332.
- (7) Arriola, D. J.; Carnahan, E. M.; Hustad, P. D.; Kuhlman, R. L.; Wenzel, T. T. *Science* **2006**, *312*, 714–719.
- (8) Wang, H. P.; Khariwala, D. U.; Cheung, W.; Chum, S. P.; Hiltner, A.; Baer, E. *Macromolecules* **2007**, *40*, 2852–2862.
- (9) Trzaska, S. T.; Lee, L. B. W.; Register, R. A. *Macromolecules* **2000**, *33*, 9215–9221.
- (10) Dounis, P.; Feast, W. J. *Polymer* **1996**, *37*, 2547–2554.
- (11) Sebastian, J. M.; Register, R. A. *J. Appl. Polym. Sci.* **2001**, *82*, 2056–2069.
- (12) Hatjopoulos, J. D.; Register, R. A. *Macromolecules* **2005**, *38*, 10320–10322.
- (13) Myers, S. B. Ph.D. Thesis, Princeton University, 2008.
- (14) Dean, D. M.; Rebenfeld, L.; Register, R. A.; Hsiao, B. S. *J. Mater. Sci.* **1998**, *33*, 4797–4812.
- (15) Register, R. A.; Bell, T. R. *J. Polym. Sci., Part B: Polym. Phys.* **1992**, *30*, 569–575.
- (16) Huang, T. C.; Toraya, H.; Blanton, T. N.; Wu, Y. *J. Appl. Crystallogr.* **1993**, *26*, 180–184.
- (17) Schrock, R. R.; Yap, K. B.; Yang, D. C.; Sitzmann, H.; Sita, L. R.; Bazan, G. C. *Macromolecules* **1989**, *22*, 3191–3200.
- (18) Lee, L. B. W.; Register, R. A. *Polymer* **2004**, *45*, 6479–6485.
- (19) Bair, H. E.; Huseby, T. W.; Salovey, R. *Polym. Prepr. (Am. Chem. Soc., Div. Polym. Chem.)* **1968**, *9* (1), 795–805.
- (20) Howard, P. R.; Crist, B. *J. Polym. Sci., Part B: Polym. Phys.* **1989**, *27*, 2269–2282.
- (21) Rangarajan, P.; Register, R. A.; Fetters, L. J. *Macromolecules* **1993**, *26*, 4640–4645.
- (22) Weimann, P. A.; Hajduk, D. A.; Chaffin, K. A.; Brodil, J. C.; Bates, F. S. *J. Polym. Sci., Part B: Polym. Phys.* **1999**, *37*, 2053–2068.
- (23) Koizumi, S.; Hasegawa, H.; Hashimoto, T. *Macromolecules* **1994**, *27*, 7893–7906.
- (24) Lee, H. H.; Register, R. A.; Hajduk, D. A.; Gruner, S. M. *Polym. Eng. Sci.* **1996**, *36*, 1414–1424.
- (25) Ward, I. M. *Mechanical Properties of Solid Polymers*, 2nd ed.; John Wiley & Sons: New York, 1983; p 333.
- (26) Brooks, N. W. J.; Mukhtar, M. *Polymer* **2000**, *41*, 1475–1480.
- (27) Hiss, R.; Hobeika, S.; Lynn, C.; Strobl, G. *Macromolecules* **1999**, *32*, 4390–4403.
- (28) Ver Strate, G.; Cozewith, C.; West, R. K.; Davis, W. M.; Capone, G. A. *Macromolecules* **1999**, *32*, 3837–3850.